Tensile Cervical Facet Capsule Ligament Mechanics:

Failure and Subfailure Responses in the Rat

Kathryn E. Lee, Andrew N. Franklin, Martin B. Davis, Beth A. Winkelstein*

Department of Bioengineering

University of Pennsylvania

Philadelphia, PA 19104

Keywords: facet joint, ligament, failure, strain, biomechanics

Word Count (Introduction through Acknowledgments): 3613

Correspondence*: Beth Winkelstein, PhD
Dept. of Bioengineering
University of Pennsylvania
120 Hayden Hall
3320 Smith Walk
Philadelphia, PA 19104-6392
215-573-4589 (phone)
215-573-2071 (fax)
winkelst@seas.upenn.edu

ABSTRACT

Clinical, epidemiological, and biomechanical studies suggest the involvement of the cervical facet joint in neck pain. Mechanical studies have suggested the facet capsular ligament to be at risk for subfailure tensile injury during whiplash kinematics of the neck. Ligament mechanical properties can be altered by subfailure injury and such loading can induce cellular damage. However, at present, there is no clear understanding of the physiologic context of subfailure facet capsular ligament injury and mechanical implications for whiplash-related pain. Therefore, this study aimed to define a relationship between mechanical properties at failure and a subfailure condition associated with pain for tension in the rat cervical facet capsular ligament. Tensile failure studies of the C6/C7 rat cervical facet capsular ligament were performed using a customized vertebral distraction device. Force and displacement at failure were measured and stiffness and energy to failure were calculated. Vertebral motions and ligament deformations were tracked and maximum principal strains and their directions were calculated. Mean tensile force at failure (2.96±0.69 N) was significantly greater ($p<0.005$) than force at subfailure (1.17±0.48 N). Mean ligament stiffness to failure was 0.75±0.27 N/mm. Maximum principal strain at failure (41.3±20.0%) was significantly higher ($p=0.003$) than the corresponding subfailure value (23.1±9.3%). This study determined that failure and a subfailure painful condition were significantly different in ligament mechanics and findings provide preliminary insight into the relationship between mechanics and pain physiology for this ligament. Together with existing studies, these findings offer additional considerations for defining mechanical thresholds for painful injuries.

INTRODUCTION

The cervical facet joint has been identified as a source of neck pain (Aprill and Bogduk, 1992; Barnsley et al. 1994) and a likely candidate for painful whiplash injury, in both clinical and biomechanical studies (Bogduk and Marsland, 1988; Kaneoka et al. 1999; Luan et al. 2000; Ono et al. 1997; Panjabi et al. 1998a,b; Pearson et al. 2004; Siegmund et al. 2001; Winkelstein et al. 1999, 2000; Yoganandan and Pintar, 1997; Yoganandan et al. 1998a, 2002). Studies of cadaveric head-neck preparations using high-speed imaging have demonstrated that the facet joint and its capsular ligament can experience excessive motions and ligament strains during whiplash simulations (Panjabi et al. 1998a,b; Pearson et al. 2004; Sundararajan et al. 2004; Yoganandan et al. 2001, 2002). Studies of isolated cervical spinal motion segments have also documented that these cervical spine kinematics can induce facet capsule stretch and possible minor ligament ruptures below the mechanical thresholds for gross failure of the ligament (Siegmund et al. 2001; Winkelstein et al. 2000). However, while these mechanical studies suggest that the facet capsular ligament may be at mechanical risk for painful injury during some neck motions, the physiologic consequence of these injuries and their relationship to the tensile mechanical response of the joint is undefined.

Tensile failure properties of the human cervical facet capsular ligament have been previously defined (Mykelbust et al. 1988; Winkelstein et al. 1999, 2000; Yoganandan et al. 2000). Mykelbust et al. (1988) reported failure forces of 112±30 N and 72±18 N for tensile loading of isolated C3/C4 and C5/C6 ligaments, respectively. Likewise, Winkelstein et al. (2000) reported ligament failure at similar forces of 94.3±44.4 N and 82.5±33.0 N for these same joints. In that study, maximum ligament distraction at failure

was 5.10±0.73 mm and 6.40±0.66 mm, respectively, producing maximum principal strains of 103.6±80.9% in the facet capsule (Winkelstein et al. 2000). In tensile failure tests of lower cervical spine specimens (C5-T1), Yoganandan et al. (2000) reported stresses of 7.4±1.3 MPa and strains of 116.0±19.6%, with corresponding stiffness and energy to failure of 36.9±6.06 N/mm and 1.5±0.4 Nm, respectively. While these studies present consistent data on the mechanical limits of the human cervical facet capsular ligament, they are unable to provide a context for investigating the effects of these mechanics on physiologic function or implications for mechanical responses at subfailure conditions.

Capsule injury prior to gross ligamentous failure has been documented in both isolated and full cervical spine specimens (Panjabi et al. 1998a; Siegmund et al. 2001; Winkelstein et al. 2000; Yoganandan et al. 2001). In cervical motion segment studies, subfailure minor ruptures were produced in the facet capsule, at strains ranging from 35.0-64.6%, for both shear and tension (Siegmund et al. 2001; Winkelstein et al. 2000). Panjabi et al. (1998b) and Pearson et al. (2004) estimated C6/C7 ligament strains during whiplash simulations to be 29.5±25.7% and 39.9±26.3%, respectively. However, these same specimens sustained ligament strains of only 6.2±5.6% for spinal motions within normal physiologic ranges (Panjabi et al. 1998b), leading these authors to suggest that whiplash injury induces ligament strains that are elevated above physiologic levels and that these elevated strains may cause ligament injury, despite lack of any evidence of rupture or noticeable injury in these specimens. All of these studies have hypothesized subfailure injuries at the microscopic level as a potential means of nociceptor activation. Nociceptive pain fibers have been identified throughout the facet joint and its capsular

47 ligament (Cavanaugh et al. 1989, 1996; McLain 1994; Inami et al. 2001).
48 Electrophysiologic studies have further shown that these fibers in the facet ligament can
49 be directly activated by tensile loading in the lumbar spine (Avramov et al. 1992;
50 Cavanaugh et al. 1989, 1996). Together, these mechanical and anatomic findings
51 suggest whiplash kinematics in the cervical spine may induce a subfailure mechanical
52 condition in the facet capsular ligament that has the potential to initiate physiologic
53 responses for pain. However, the relationship between the magnitude of relevant
54 subfailure and failure injury mechanics in the context of physiologic outcomes remains
55 unknown.

56 Our laboratory has developed an *in vivo* model of facet joint distraction in the rat
57 for investigating the physiologic sequelae of pain produced from this loading (Lee et al.
58 2004a,b). That model enables repeatable and controlled distraction across the facet joint
59 and its capsular ligament. Vertebral distractions of 0.57±0.11 mm in that model are
60 adequate for producing repeatable behavioral sensitivity and pain symptoms (as measured
61 by mechanical allodynia) (Lee et al. 2004a). Such joint distractions produce strains in the
62 C6/C7 facet capsule of 27.7±11.9% (Lee et al. 2004a). While no observable rupture of
63 the ligament is produced at these magnitudes of vertebral distraction, information about
64 the relative mechanical severity of this subfailure condition compared to failure remains
65 to be determined.

66 Therefore, the goal of the present study is to characterize the failure and
67 subfailure mechanical properties of the rat cervical facet capsular ligament in tension.
68 The subfailure condition selected here is defined as 0.57 mm of vertebral distraction,
69 based on previous *in vivo* studies in which this distraction predictably produced

behavioral sensitivities sustained over time as persistent pain (Lee et al. 2004a). It is hypothesized that for this ligament, the corresponding subfailure tensile condition that produces pain in the *in vivo* model is mechanically distinct from ligament failure, despite being sufficient to cause physiologic manifestation of pain. Characterization of the mechanical properties of this ligament and the relationship between its failure and subfailure loading will provide context for understanding both the mechanical and physiologic responses of injuries to this joint as well as other ligaments.

METHODS

Specimen Preparation & Loading Procedure

Male Holtzman rats (n=11), weighing 325-425 g, were used in this study. All experimental procedures were approved by the University of Pennsylvania Institutional Animal Care and Use Committee and carried out according to the guidelines of the Committee for Research and Ethical Issues of the International Association for the Study of Pain (Zimmermann 1983). Rats were euthanized by $C0_2$ inhalation and cervical spinal motion segments from C4-T2 were immediately removed *en bloc*. Specimens were cleared of all musculature. The laminae, facet joints, and spinous processes at C6/C7 were exposed bilaterally under a surgical microscope (Carl Zeiss Inc., Thornwood, NY). Tensile loading was performed using a customized device; distraction methods were identical to previous *in vivo* investigations (Lee et al. 2004a,b). Briefly, the supraspinous ligament, interspinous ligament, and ligamentum flavum were bilaterally resected at C6/C7 to enable specimen attachment, fixation, and loading during testing. In addition, for this study, the left capsular ligament, both longitudinal ligaments, and the

intervertebral disc at C6/C7 were transected and removed, to enable isolation of the right facet capsular ligament only. The C6 and C7 spinous processes were rigidly attached to the distraction device by microforceps (Figure 1); C7 was held fixed and C6 was translated rostrally using a manual micrometer (Newport Corp., Irvine, CA). A linear variable differential transducer (LVDT) (MicroStrain Inc., Burlington, VT; 0.160 μm resolution) and load cell (Interface Inc., Scottsdale, AZ; 0.02 N resolution) were rigidly coupled to the C6 microforceps and their synchronized data were acquired at 10 Hz. LVDT displacement histories were used to calculate distraction rates. Displacements were applied until gross ligament failure was observed both visually and by a decrease in tensile force.

The right facet joint and capsular ligament were imaged during distraction at 6 fps using a digital video camera (QImaging, B.C. Canada), with 1280 x 1024 pixel resolution. Image data were synchronized with the transducer data and acquired using LabVIEW (National Instruments, Corp., Austin, TX). Polystyrene magnetic particles (diameter of 0.17±0.01 mm; Spherotech, Inc., Libertyville, IL) were affixed to the bones and ligament to track joint motions. Particles were placed on each of the C6 and C7 laminae, as vertebral markers, to track bony motions across the joint (Figure 2). To calculate ligament strains, nine additional particles, serving as ligament markers, were placed on the posterior surface of the C6/C7 capsular ligament in a 3 x 3 grid, creating 4 elements (Figure 2). Ligament regions were defined by quadrants of the grid: Quadrant I (QI) as caudal-medial; Quadrant II (QII) as rostral-medial; Quadrant III (QIII) as caudal-lateral; Quadrant IV (QIV) as rostral-lateral.

Data Analysis

Force at failure was measured as the maximum force at ligament failure. Based on the force-displacement response, ligament failure was defined as a drop in force with increased displacement. For each specimen, visual inspection of the ligament confirmed the existence and site of failure (Figure 3). Stiffness to failure was calculated as the slope of the force-displacement curve from 20-100% of the peak force, which represented the most linear portion of the curve for all specimens (Figure 4). Energy to failure was calculated as the area under the force-displacement curve up to the point of failure.

Image tracking software (Image Pro Plus; Media Cybernetics Inc, Silver Spring, MD) located all vertebral and ligament marker centroids for each frame up to and including failure. Vertebral distraction was defined as the linear displacement, in the rostral (x) direction, of the C6 vertebral marker relative to the C7 vertebral marker. This procedure has previously been shown to produce distraction primarily in the rostral-caudal direction (x-axis, Figure 2), with negligible motion in the medial-lateral direction (y-axis, Figure 2) (Lee et al. 2004a,b). Initial positions of the ligament markers, prior to loading, were used to construct a finite element mesh of 4 shell elements in LS-DYNA (LSTC, Livermore, CA). The mesh divided the ligament into four quadrants (Quadrants I-IV) (Figure 2), which were used to describe the location of maximum principal strain and failure. The positional coordinates of ligament markers during distraction sequences were used to calculate the corresponding displacement fields and Lagrangian strains within the plane of the elements. For each specimen, maximum principal strain and maximum shear strain in the ligament were calculated.

Matched force and strain data were also examined for each specimen at a joint distraction corresponding to the subfailure value at vertebral distraction of 0.57 mm (Figure 3). All mechanical data at this vertebral distraction were analyzed in the same manner as the failure data for comparison. One specimen (#77) did not reach this vertebral distraction prior to its ligament rupture. As such, subfailure data from this specimen were not available for analysis.

Statistical Analysis

Vertebral distraction, tensile force, maximum principal strains and directions, and shear strains in the ligament were tested for normality using the Shapiro-Wilk test and compared between failure and subfailure conditions using a paired Student's t-test (Zar, 1999). Because Specimen #77 did not reach 0.57 mm of distraction prior to failure, its data were excluded for all statistical comparisons between failure and subfailure. All statistical analyses were performed using SYSTAT (SYSTAT Software Inc., Richmond, CA) and significance was defined as $p<0.05$.

RESULTS

There was no significant departure from normality for any of the mechanical parameters (vertebral distraction, tensile force, maximum principal strain and direction, maximum shear strain) for either condition (failure, subfailure). For these studies, the average rate of distraction was 0.08±0.02 mm/s. The mean tensile force at failure was 2.96±0.69 N, corresponding to a vertebral distraction of 1.52±0.76 mm (Table 1). Digitization errors were 0.006±0.001 mm, only 0.4% of the imposed vertebral

161 distractions. As such, errors did not contribute substantially to calculated distraction.
162 Linear regression fits to force-displacement data had a mean R^2 value of 0.96±0.03. The
163 mean C6/C7 facet capsular ligament stiffness to failure was 0.75±0.27 N/mm and mean
164 energy to failure was 0.008±0.005 Nm (Figure 4, Table 1). For all specimens, force
165 demonstrated a steady increase with increasing displacement until failure was reached.

166 At ligament failure, the mean maximum principal strain in the capsule was
167 41.3±20.0% (Figure 5, Table 2). The maximum principal strain was located in each of
168 the quadrants QI, QII, QIII and QIV (Table 2). The mean maximum shear strain in the
169 capsule was 23.1±10.9%, and was significantly smaller than the corresponding maximum
170 principal strain ($p=0.003$). Errors in determining strains were small, and had an average
171 value of 1.3±1.2%. Visual inspection of the ligaments confirmed that, for all cases, the
172 site of gross failure was located in the same quadrant (anatomic region of ligament) as the
173 site of maximum principal strain. Directions associated with the maximum principal
174 strains were oriented at a mean angle of 3.1±41.2˚ off the x-axis (Figure 5B, Table 2). In
175 7 of the 11 specimens, ligament failures occurred as a small tear forming in the ligament
176 midsubstance immediately prior to failure and progressing until failure.

177 Subfailure vertebral distraction of 0.57±0.01 mm produced 1.17±0.48 N of mean
178 tensile load. The magnitude of subfailure distraction and force were significantly lower
179 than their corresponding values at failure ($p<0.005$, both cases). Mean maximum
180 principal strain at this condition was 23.1±9.3%, which was also significantly smaller
181 ($p=0.003$) than maximum strain in the ligament at failure (Figure 5). Vectors describing
182 directions of maximum principal strain at subfailure were oriented at 28.5±16.9˚ relative
183 to the x-axis (Figure 5D, Table 2), and were not significantly different from those at

failure ($p=0.06$). The mean maximum shear strain at subfailure was 6.9±7.9%, which was significantly smaller than the corresponding maximum principal strain at subfailure and the maximum shear strain at failure ($p<0.005$, both cases). For all specimens except Specimen #77, no gross ligament damage was visible at subfailure. While Specimen #77 failed at a vertebral distraction of 0.43 mm (Table 1), it ruptured in a similar manner as the majority of the other specimens, with a small tear in the midsubstance.

DISCUSSION

While tensile failure properties of human cervical facet capsular ligaments have been previously reported (Mykelbust et al. 1988; Winkelstein et al. 1999, 2000; Yoganandan et al. 2000), this study is the first to report failure or subfailure properties for this ligament in the rodent. Mechanical studies have shown increased joint laxity, decreased ligament stiffness, and an overall change in the force-displacement response of various ligaments after subfailure loading in human and rabbit tissue (Panjabi et al. 1996, 2001; Pollock et al. 2000). These reports suggest that subfailure loading may produce microscopic ligament damage, in turn affecting the subsequent mechanical properties of the ligament. Histologic study of the rat medial collateral ligament after subfailure injury revealed necrosis associated with strains significantly below those necessary to induce structural damage (Provenzano et al. 2002), implying that cellular damage can be induced without corresponding observable ligament rupture. These mechanical and histologic reports suggest that the subfailure condition applied in this study may lead to microscopic damage, potentially altering the mechanical function of this ligament and may be sufficient to produce pain symptoms. Tensile failure studies of cadaveric facet capsular

ligaments have reported a distinct drop in the force-displacement curve prior to frank ligament rupture (Siegmund et al. 2001; Winkelstein et al. 2000); strains sustained at these minor failures were 62% of failure values (Winkelstein et al. 2000). The current study reports maximum principal strains at subfailure that are 56% of the corresponding failure values for rupture of the ligament. Our study also found the subfailure tensile force to be 40% of the failure force, which agrees with the corresponding force at initial failure in the human cadaveric ligament which was found to be 47% of the peak force for combined bending and shear (Siegmund et al. 2001). While mechanical scaling relationships between the rat and the human remain undefined and may present an experimental challenge, present findings demonstrate similar relative relationships exist for this ligament's mechanical properties at failure and subfailure in both the rat and the human. This adds further relevance to the *in vivo* findings related to the mechanical injuries producing pain. Continued efforts are needed to develop an appropriate scaling factor between the rat and the human for comparing mechanical data in these and other species.

In our study, maximum principal strains in the ligament were generally directed across the joint line, parallel to the direction of applied distraction, along the spine's long axis. This suggests that the ligamentous fibers may be oriented across the joint line, although additional mechanical and histologic studies are necessary to fully quantify the orientation of ligament fibers and the precise mode of this ligament's failure. Previous work has demonstrated tensile failure occurring primarily in the midsubstance of human cadaveric facet capsular ligaments (Winkelstein et al. 2000). Likewise, the current study reports ligament failures as small tears in the midsubstance, primarily occurring in the

medial portion of the capsule (QI and QII). While ligament deformation and strain are not dependent on loading rate, peak load and stiffness at failure do depend on rate and are higher for fast-rate loading (Winkelstein et al. 1999; Yoganandan et al. 1998b). As such, the strain data reported here for quasistatic loading likely reflect those maximum principal strains induced in the ligament for other loading rates. However, the location of rupture may be altered for other loading rates. The distraction method used in this study is purely tensile and does not fully model the coupled motions of all physiologic modes of loading. Indeed, similar approaches for strain measurement have been implemented recently for the human lumbar facet capsule and report both a dependence on loading direction and subfailure mechanical responses for this ligament (Ianuzzi et al. 2004; Little and Khalsa, 2005). Accordingly, capsule strains reported in this study may not be representative of those experienced during other physiologic motions.

The subfailure vertebral distraction magnitude selected in this study was based on existing *in vivo* facet distraction-mediated pain models and cadaveric data obtained during whiplash simulations (Lee et al. 2004a, Panjabi et al. 1998b, Pearson et al. 2004). *In vivo* tensile vertebral distractions matching those applied in the current study have been previously demonstrated to produce ligament strains (27.7±11.9%) (Lee et al. 2004b) that are similar to those produced in the C6/C7 ligament (29.5-39.9%) during whiplash simulations (Panjabi et al. 1998b, Pearson et al. 2004). These *in vivo* vertebral distractions elicited behavioral sensitivity, which remained elevated above physiologic levels for 14 days (Lee et al. 2004a). Moreover, significantly increased astrocytic activation was also observed in the spinal cord of these rats after these subfailure vertebral distractions (Lee et al. 2004a), suggesting sustained cellular reactivity for this

253 loading. The vertebral distractions in the present subfailure study produced ligament
254 strains of 23.1±9.3% (Table 2) that are similar to those produced *in vivo* causing pain. In
255 fact, in directly comparing the strain data from the current study with the previously
256 reported *in vivo* work, a Student's t-test reveals no statistical difference ($p=0.42$). This
257 suggests that the subfailure ligament distractions used here are sufficient to produce pain
258 symptoms in an *in vivo* condition. It should be noted, however, that while the current
259 study involved unilateral facet capsule distraction, the distraction applied in the *in vivo*
260 study was applied across both the right and left capsules. Demonstration of the presence
261 of nociceptors (Cavanaugh et al. 1989, 1996; Inami et al. 2001; McLain 1994) and their
262 activation (Avramov et al. 1992; Cavanaugh et al. 1996) in the ligament further suggests
263 a role for this joint in pain signaling. Given the histologic and electrophysiologic
264 evidence of this ligament's involvement in nociception, the current study suggests that
265 subfailure tensile loading of the ligament may lead to nociceptive physiologic changes in
266 the spine, despite lack of its mechanical injury.

267 Visual inspection of image data at subfailure revealed no evidence of ligamentous
268 damage. However, it remains unclear whether subfailure loading at this magnitude
269 produces small, or even microscopic tears, which would not be visible to the naked eye.
270 As such, while this study did not histologically examine the ligament for evidence of
271 damage at subfailure, we have previously demonstrated that stiffness is not altered for
272 repeated distraction at these levels (Franklin et al. 2004), suggesting no gross structural
273 damage occurs at these distraction levels. Further mechanical or histologic investigations
274 of the ligament would provide further characterization and interpretation of the
275 mechanical and physiologic meaning of these loading conditions. Of note, while tensile

failure of cadaveric ligaments has been reported to produce a noticeable subfailure event in the force-displacement curve during loading (Siegmund et al. 2001; Winkelstein et al. 2000), such a distinct event was not detected at any point in the loading responses for the ligaments in this study (Figure 4). This suggests that the mechanical response of the fibers within the rat ligament may be different than that of the matched human ligament. Also, while Specimen #77 failed prior to its reaching the subfailure value, its structural properties at failure were within the range of the values determined for the other specimens (Table 2).

The findings presented here offer a foundation for interpreting existing physiologic data obtained during subfailure ligament distraction (Lee et al. 2004a). Data show that for this subfailure distraction condition, ligament forces and strains are significantly smaller than those produced at failure, suggesting no structural damage at these levels and that this subfailure distraction in an *in vivo* setting is not sufficient to produce gross injury. However, in the context of *in vivo* work (Lee et al. 2004a), this subfailure condition *does* produce sustained cellular responses in the spinal cord and pain symptoms, suggesting a threshold for physiologic damage or nociceptive modulation at this level of mechanical loading for this joint. While distractions may not produce detectable alteration in mechanical responses for the rat facet capsular ligament, they may indeed be sufficient to trigger the physiologic sequelae of pain and its symptoms. This study provides context for existing physiologic data obtained at subfailure levels, offers new insight into mechanical thresholds of facet joint injury, and lays the groundwork for further investigation into the physiologic implications of this and other subfailure conditions in ligamentous loading.

ACKNOWLEDGMENTS

This work was funded by grant support from the Whitaker Foundation (RG-02-0311), the Catharine D. Sharpe Foundation, and a graduate fellowship from the National Science Foundation.

REFERENCES

April, C., Bogduk, N., 1992. The prevalence of cervical zygapophyseal joint pain. Spine 17, 744-747.

Avramov, A.I., Cavanaugh, J.M., Ozaktay, C.A., Getchell, T.V., King, A.I., 1992. The effects of controlled mechanical loading on group-II, III, and IV afferent units from the lumbar facet joint and surrounding tissue. The Journal of Bone & Joint Surgery 74-A, 1464-1471.

Barnsley, L., Lord, S., Bogduk, N., 1994. Whiplash injury. Pain 58, 283-307.

Bogduk, N., Marsland, A., 1988. The cervical zygapophysial joints as a source of neck pain. Spine 13, 610-617.

Cavanaugh, J.M., El-Bohy, A., Hardy, W.N., Getchell, T.V., Getchell, M.L., King, A.I., 1989. Sensory innervation of soft tissues of the lumbar spine in the rat. Journal of Orthopaedic Research 7, 378-388.

Cavanaugh, J.M., Ozaktay, A.C., Yamashita, H.T., King, A.I., 1996. Lumbar facet pain: biomechanics, neuroanatomy, and neurophysiology. Journal of Biomechanics 29, 1117-1129.

Franklin, A.N., Lee, K.E., Winkelstein, B.A., 2004. Tensile Mechanical Characterization of the Rat Facet Capsule. Biomedical Engineering Society Annual Fall Meeting, Philadelphia, PA.

Ianuzzi, A., Little, J.S., Chiu, J.B., Baitner, A., Kawchuk, G., Khalsa, P.S., 2004. Human lumbar facet joint capsule strains: I. During physiological motions. The Spine Journal 4, 141-152.

Inami, S., Shiga, T., Tsujino, A., Yabuki, T., Okado, N., Ochiai, N., 2001. Immunohistochemical demonstration of nerve fibers in the synovial fold of the human cervical facet joint. Journal of Orthopaedic Research 19, 593-596.

Kaneoka, K., Ono, K., Inami, S., Hayashi, K., 1999. Motion analysis of cervical vertebrae during whiplash loading. Spine 24, 763-770.

Lee, K.E., Davis, M.B., Mejilla, R.M., Winkelstein, B.A., 2004a. *In vivo* cervical facet capsule distraction: mechanical implications for whiplash and neck pain. Proceedings of the 48th Stapp Car Crash Conference, 373-395, Paper # 2004-22-0016.

Lee, K.E., Thinnes, J.H., Gokhin, D.S., Winkelstein, B.A., 2004b. A novel rodent neck pain model of facet-mediated behavioral hypersensitivity: implications for persistent pain and whiplash injury. Journal of Neuroscience Methods 137, 151-159.

Little, J.S., Khalsa, P.S., 2005. Material properties of the human lumbar facet joint capsule. Journal of Biomechanical Engineering 127, 15-24.

Luan, F., Yang, K.H., Deng, B., Begeman, P.C., Tashman, S., King, A.I., 2000. Qualitative analysis of neck kinematics during low-speed rear-end impact. Clinical Biomechanics 15, 649-657.

McLain, R.F., 1994. Mechanoreceptor endings in human cervical facet joints. Spine 19, 495-501.

Mykelbust, J.B., Pintar, F., Yoganandan, N., Cusick, J.F., Maiman, D., Myers, T.J., Sances, A., Jr., 1988. Tensile strength of spinal ligaments. Spine 13, 526-531.

Ono, K., Kaneoka, K., Wittek, A., Kajzer, J., 1997. Cervical injury mechanism based on the analysis of human cervical vertebral motion and head-neck-torso kinematics during low speed rear impacts. Proceedings of the 41st Stapp Car Crash Conference, 339-356, Paper #973340.

Panjabi, M.M., Yoldas, E., Oxland, T.R., Crisco, J.J., 3rd., 1996. Subfailure injury of the rabbit anterior cruciate ligament. Journal of Orthopaedic Research 14, 216-222.

Panjabi, M.M., Pearson, A.M., Ito, S., Ivancic, P.C., Wang, J.-L., 1998a. Cervical spine curvature during simulated whiplash. Clinical Biomechanics 19, 1-9.

Panjabi, M.M., Cholewicki, J., Nibu, K., Grauer, J.N., Vahldiek, M., 1998b. Capsular ligament stretches during in vitro whiplash simulations. Journal of Spinal Disorders 11, 227-232.

Panjabi, M.M., Courtney, T.W., 2001. High-speed subfailure stretch of rabbit anterior cruciate ligament: changes in elastic, failure, and viscoelastic characteristics. Clinical Biomechanics 16, 334-340.

Pearson, A.M., Ivancic, P.C., Ito, S., Panjabi, M.M., 2004. Facet joint kinematics and injury mechanisms during simulated whiplash. Spine 29, 390-397.

Pintar, F.A., Yoganandan, N., Myers, T. Elhagedib, A., Sances, A., 1992. Biomechanical properties of human lumbar spine ligaments. Journal of Biomechanics 25, 1351-1356.

Pollack, R.G., Wang, V.M., Bucchieri, J.S., Cohen, N.P., Huang, C.Y., Pawluk, R.J., Flatow, E.L., Bigliani, L.U., Mow, V.C., 2000. Effects of repetitive subfailure strains on the mechanical behavior of the inferior glenohumeral ligament. Journal of Shoulder & Elbow Surgery 9, 427-435.

Provenzano, P.P., Heisey, D., Hayashi, K., Lakes, R., Vanderby, R., Jr., 2002. Subfailure damage in ligament: a structural and cellular evaluation. Journal of Applied Physiology 92, 362-371.

Siegmund, G.P., Myers, B.S., Davis, M.B., Bohnet, H.F., Winkelstein, B.A., 2001. Mechanical evidence of cervical facet capsule injury during whiplash. Spine 26, 2095-2101.

Sundararajan, S., Prasad, P., Demetropoulos, C.K., Tashman, S., Begeman, P.C., Yang, K.H., King, A.I., 2004. Effect of head-neck position on cervical facet stretch of post mortem human subjects during low speed rear end impacts. Proceedings of the 48th Stapp Car Crash Conference, 331-372, Paper #2004-22-0015.

Winkelstein, B.A., Nightingale, R.W., Richardson, W.J., Myers, B.S., 1999. Cervical facet joint mechanics: its application to whiplash injury. Proceedings of the 43rd Stapp Car Crash Conference, 243-252, Paper # 99SC15.

Winkelstein, B.A., Nightingale, R.W., Richardson, W.J., Myers, B.S., 2000. The cervical facet capsule and its role in whiplash injury. Spine 25, 1238-1246.

Yoganandan, N., Pintar, F.A., 1997. Inertial loading of the human cervical spine. Journal of Biomechanical Engineering 119, 237-240.

Yoganandan, N., Pintar, F.A., Klienberger, M., 1998a. Cervical spine vertebral and facet joint kinematics under whiplash. Journal of Biomechanical Engineering 120, 305-307.

Yoganandan, N., Pintar, F.A., Kumaresan, S., 1998b. Biomechanical assessment of human cervical spine ligaments. Proceedings of the 42nd Stapp Car Crash Conference, 223-236, Paper #983159.

Yoganandan, N., Kumaresan, S., Pintar, F.A., 2000. Geometric and mechanical properties of human cervical spine ligaments. Journal of Biomechanical Engineering 122, 623-629.

Yoganandan, N., Cusick, J.F., Pintar, F.A., Rao, R.D., 2001. Whiplash injury determination with conventional spine imaging and cryomicrotomy. Spine 26, 2443-2448.

Yoganandan, N., Pintar, F.A., Cusick, J.F., 2002. Biomechanical analyses of whiplash injuries using an experimental model. Accident Analysis and Prevention 34, 663-671.

Zar, J.H., 1999. Biostatistical Analysis. Prentice-Hall, Inc., Upper Saddle River, NJ.

Zimmermann M., 1983. Ethical guidelines for investigations of experimental pain in conscious animals. Pain 16, 109-110.

Table 1. Summary of failure properties of isolated rodent facet capsules.

Specimen	Weight (g)	Vertebral Distraction (mm)	Tensile Load (N)	Tensile Stiffness (N/mm)	Energy at Failure (Nm)
52	326	1.88	3.56	0.99	0.006
75	404	1.03	2.51	0.68	0.005
76	404	3.40	3.92	0.51	0.016
77	346	0.43	2.47	1.05	0.003
78	392	0.92	3.75	1.21	0.006
79	418	1.09	2.52	0.77	0.005
112	398	1.56	2.86	0.42	0.008
114	392	1.37	3.81	0.63	0.019
115	410	1.72	2.98	1.00	0.006
116	396	1.47	2.17	0.55	0.007
117	368	1.89	2.04	0.43	0.010
Average (SD)	**391 (26)**	**1.52 (0.76)**	**2.96 (0.69)**	**0.75 (0.27)**	**0.008 (0.005)**

Table 2. Summary of capsule strain data.

	FAILURE				SUBFAILURE		
Specimen	**Maximum Principal Strain (%)**	**Maximum Principal Strain Direction (relative to x-axis) (°)**	**Maximum Shear Strain (%)**	**Location of Maximum Principal Strain (Quadrant)**	**Maximum Principal Strain (%)**	**Maximum Principal Strain Direction (relative to x-axis) (°)**	**Maximum Shear Strain (%)**
52	47.8	45.0	33.2	I	21.9	25.7	11.0
75	38.1	9.8	15.4	I	37.2	57.9	15.5
76	64.4	-36.2	44.6	IV	15.8	10.1	3.5
77	19.9	23.5	11.2	II	*	*	*
78	27.2	26.6	20.9	IV	17.3	25.0	14.4
79	55.1	30.3	26.2	II	34.9	20.1	15.0
112	32.6	-89.4	5.1	IV	15.3	54.3	-9.8
114	36.0	43.4	25.9	III	30.2	29.1	6.2
115	83.9	12.7	22.2	I	30.8	3.8	5.3
116	18.4	6.5	18.7	II	11.2	30.4	-0.6
117	31.0	-37.5	31.1	II	16.7	28.8	8.5
Average (SD)	**41.3 (20.0)**	**3.14 (41.2)**	**23.1 (10.9)**	**-**	**23.1 (9.3)**	**28.5 (16.9)**	**6.9 (7.9)**

* Subfailure data not available for Specimen #77, as it failed prior to reaching subfailure distraction.

Figure Legends

Figure 1. Facet distraction device, with microforceps, micrometer, LVDT, and load cell. A surgical microscope is mounted above the setup to acquire image data. For distraction, the C7 microforceps are held rigidly in place while the C6 microforceps are translated rostrally, using the micrometer.

Figure 2. Schematic illustrating the posterior view of the C6/C7 facet joint and its capsule (**A**). Two sets of markers are used: vertebral markers (large circles) are placed on the C6 and C7 laminae to track bony motions and nine ligament markers (small circles) are placed on the facet capsular ligament and define a grid for finite element analysis. The grid contains four quadrants, labeled I-IV. A representative image is also shown for a typical ligament exposure (Specimen #52), demonstrating the relevant markers and anatomy (**B**). X- and y- directions are shown in (**A**) for reference.

Figure 3. A series of *ex vivo* images obtained during tensile failure. In the reference condition (**A**), the vertebral separation is represented by x. Vertebral distraction is calculated using the x-coordinate of each vertebral marker. Subfailure vertebral distraction (**B**) is calculated as ($x_{sf} - x$) and vertebral distraction at failure (**C**) was calculated as ($x_f - x$). This test specimen (#52) sustained vertebral distractions of 0.57 mm and 1.88 mm for subfailure and failure, respectively; maximum principal strains in the capsule were 17.3% (subfailure) and 27.2% (failure). The location of failure occurred in Quadrant I (**C**) and is indicated by an arrow.

Figure 4. A representative force-displacement curve (Specimen #78) indicating ligament failure. The linear regression fit (R^2=0.98) to the data between 20-100% of failure load estimates the capsule stiffness to failure. Failure occurred at 3.75 N, with a stiffness of 1.21 N/mm.

Figure 5. Representative maximum principal strains in the capsular ligament (Specimen #78) at failure (maximum 27.2%) (**A**) and subfailure (maximum 17.3%) (**C**). Also shown are the corresponding direction vectors of these strains for failure (**B**) and subfailure (**D**), indicating the primary direction across the joint. Quadrants I-IV are shown in (**A**) for reference. For this specimen, failure occurred as a midsubstance tear in QIV, corresponding to the location of maximum strain in (**A**).

Figure 1

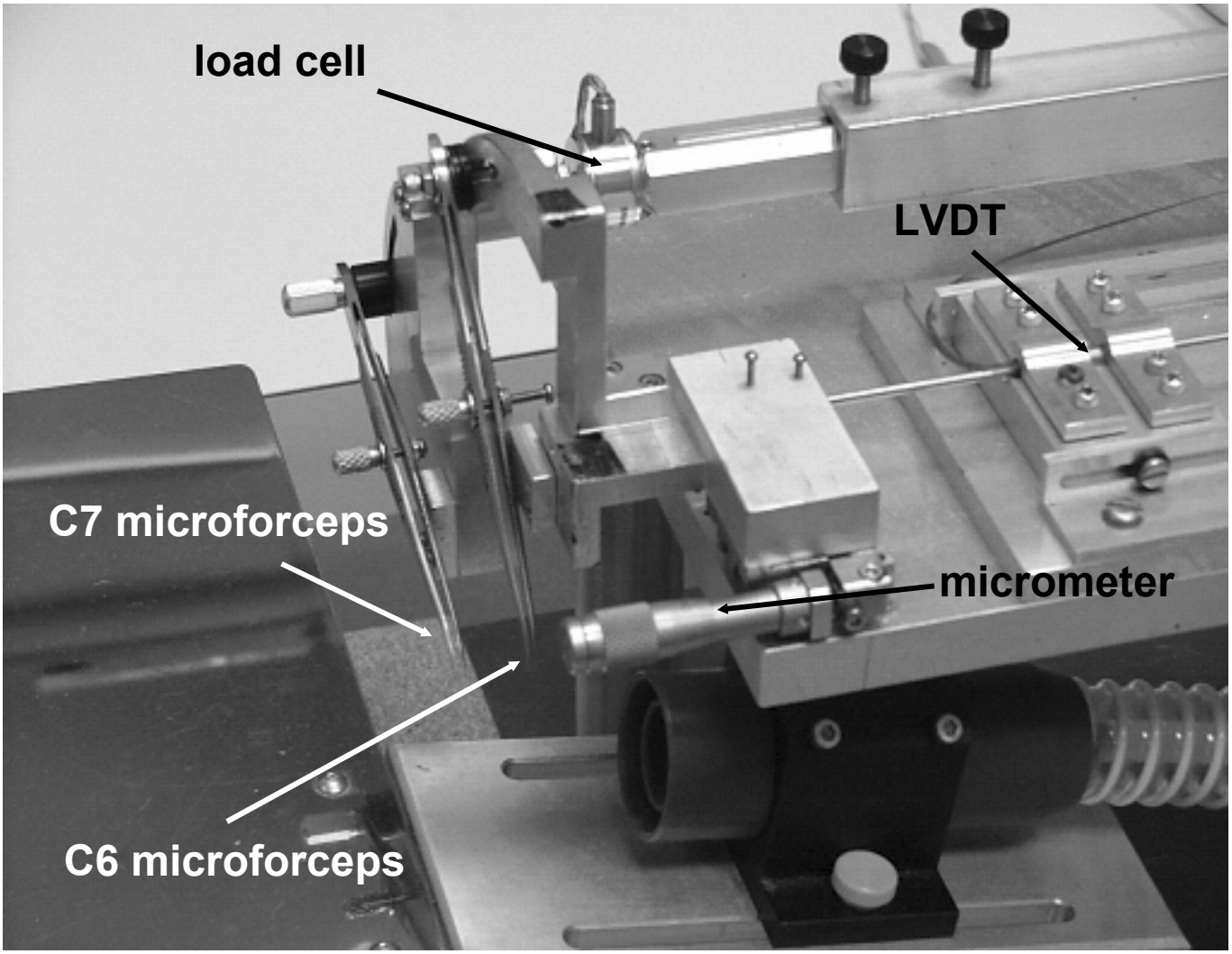
load cell
LVDT
C7 microforceps
micrometer
C6 microforceps

Figure 2

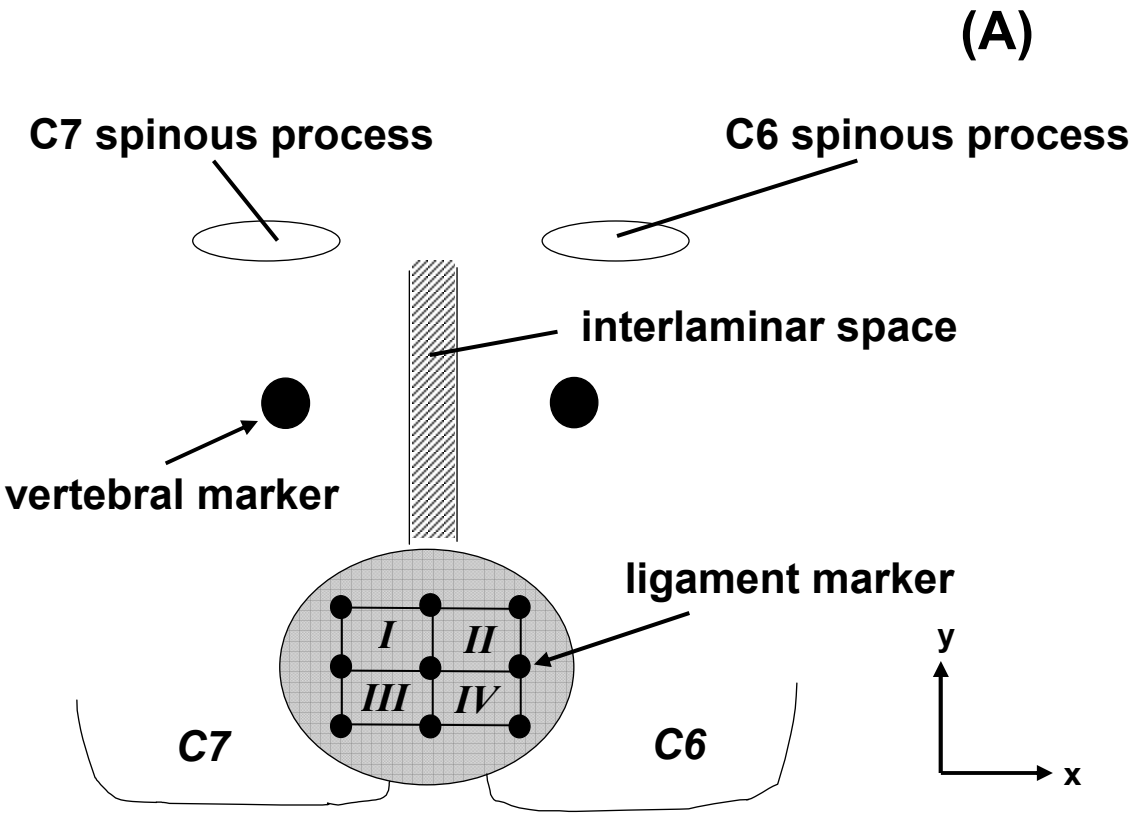
(A)
C7 spinous process
C6 spinous process
interlaminar space
vertebral marker
ligament marker
I
II
III
IV
C7
C6
y
x

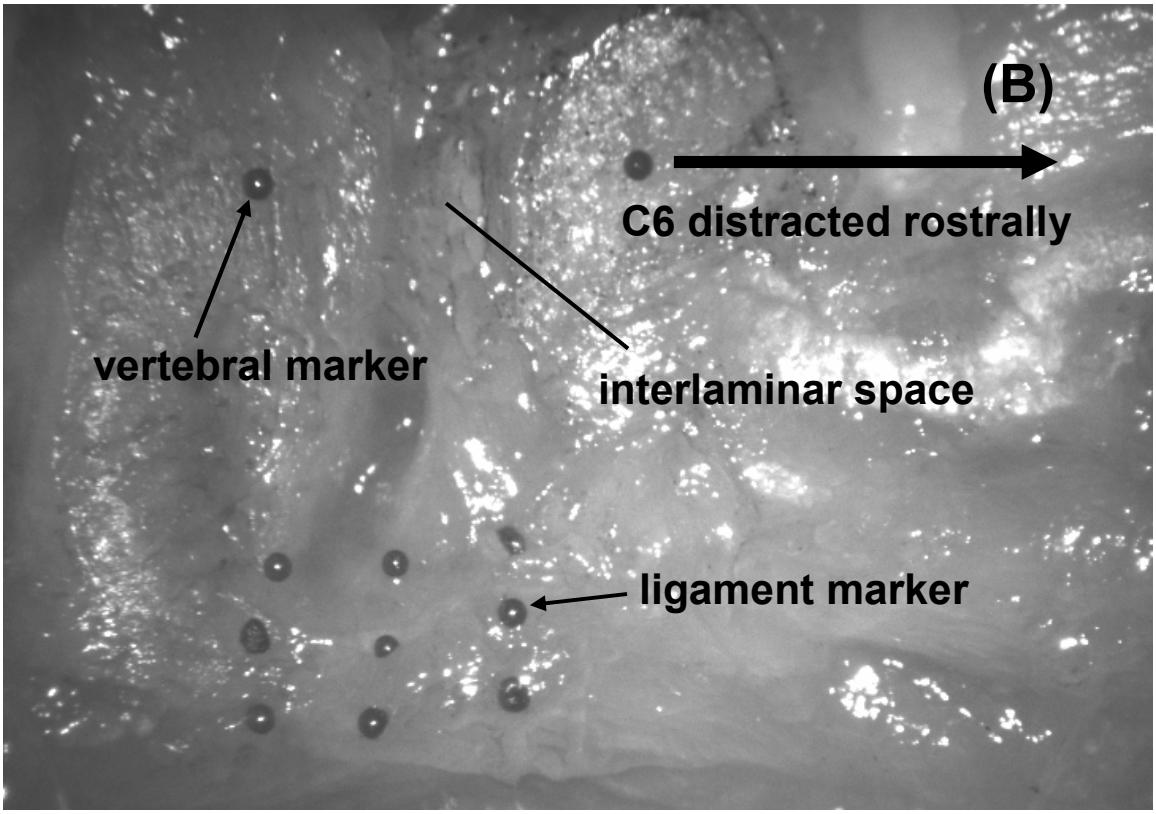
(B)
C6 distracted rostrally
vertebral marker
interlaminar space
ligament marker

Figure 3

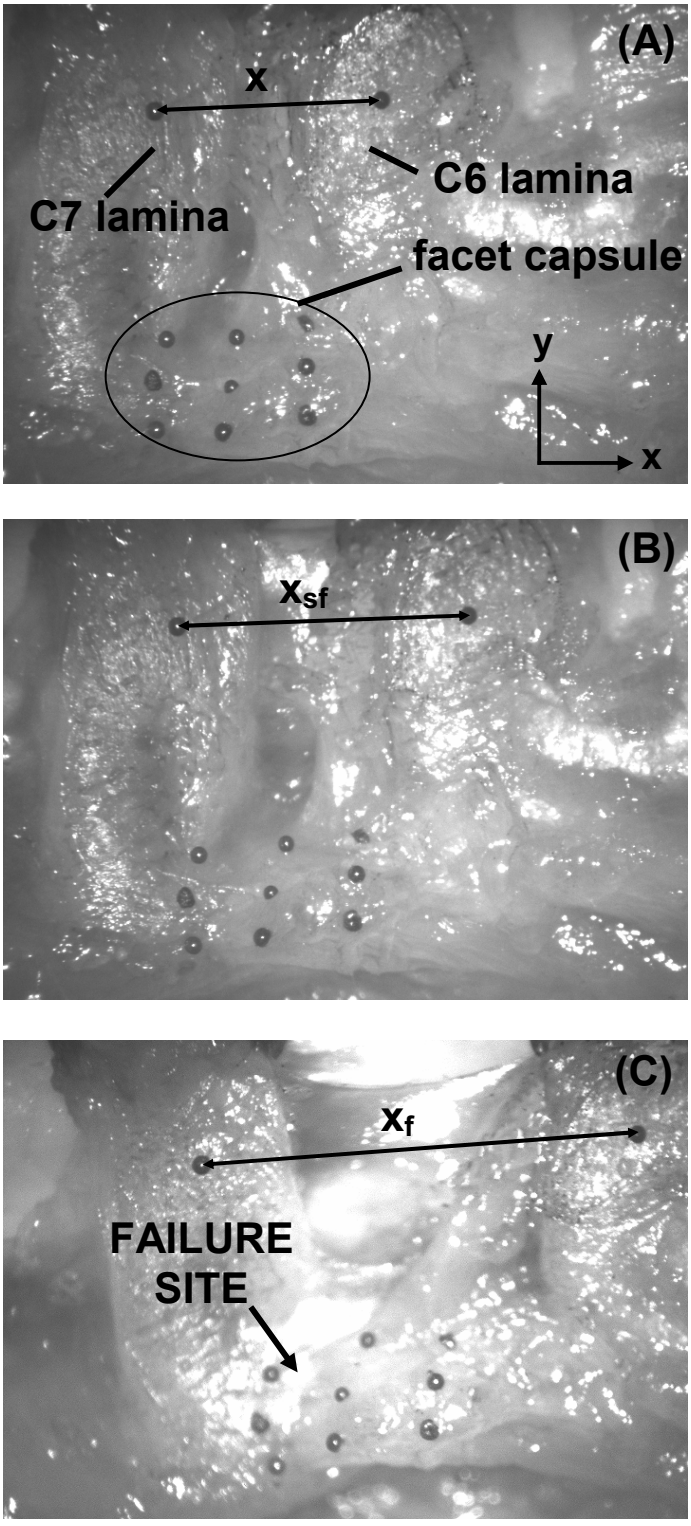
(A)
x
C7 lamina
C6 lamina
facet capsule
y
x
(B)
x_{sf}
(C)
x_f
FAILURE
SITE

Figure 4

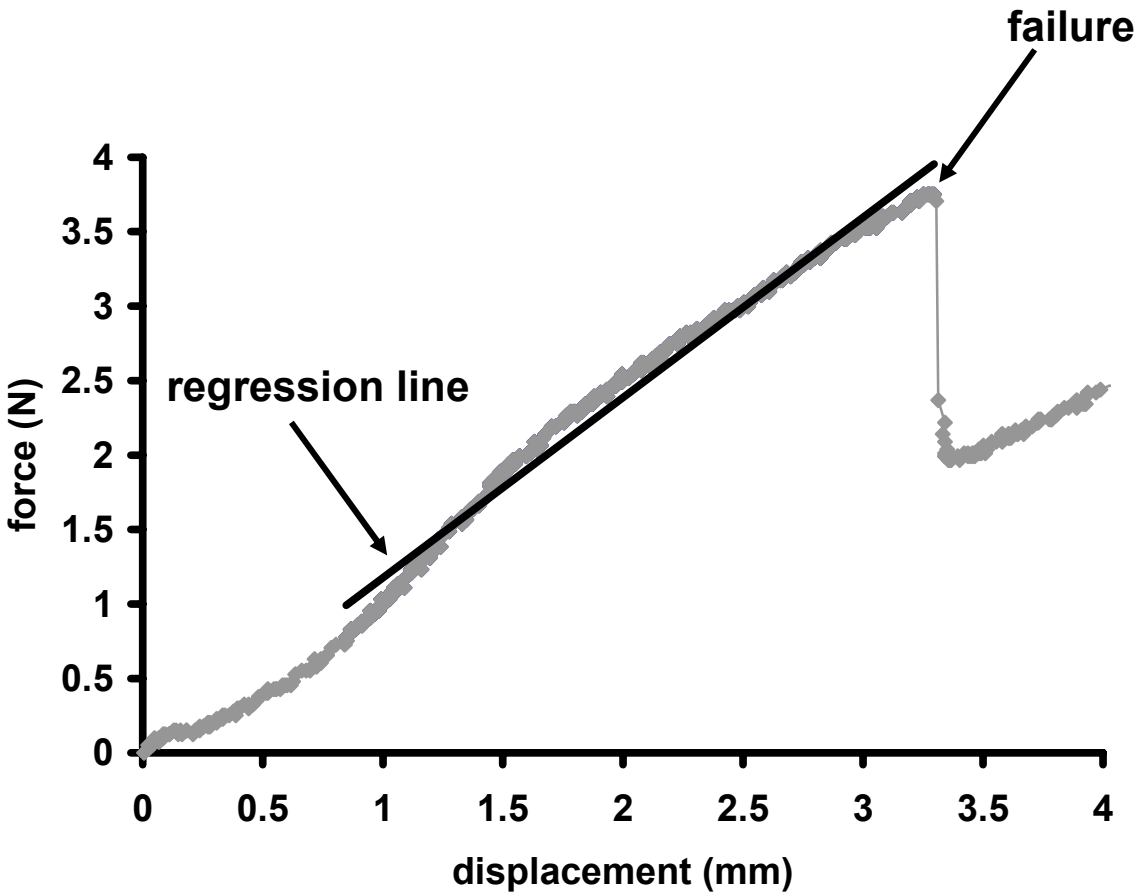
failure
regression line
force (N)
displacement (mm)
0
0.5
1
1.5
2
2.5
3
3.5
4

Figure 5

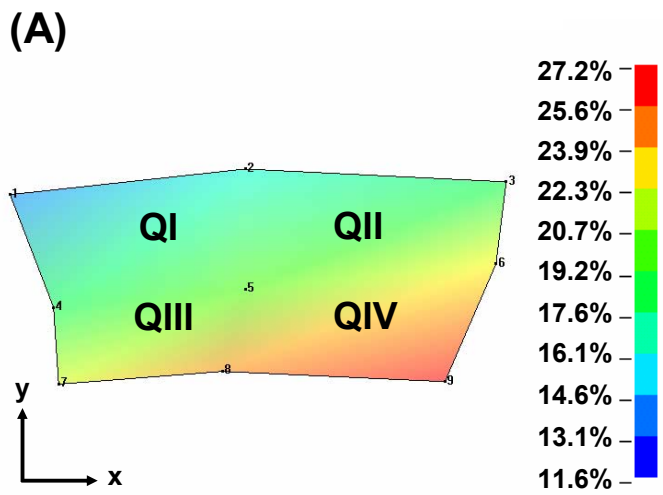
(A)
QI
QII
QIII
QIV
27.2%
25.6%
23.9%
22.3%
20.7%
19.2%
17.6%
16.1%
14.6%
13.1%
11.6%
y
x

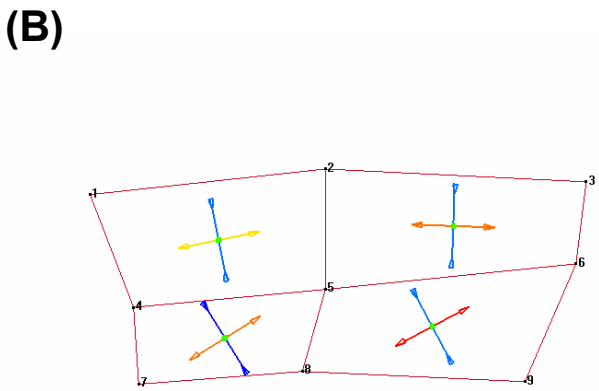
(B)

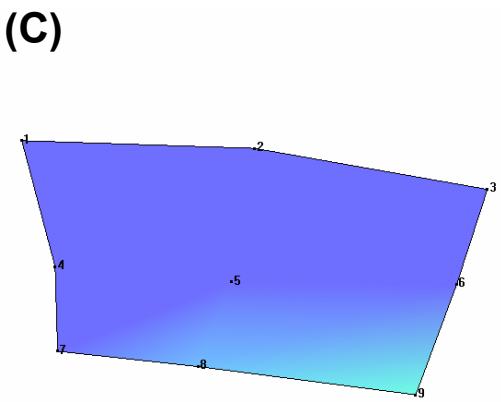
(C)

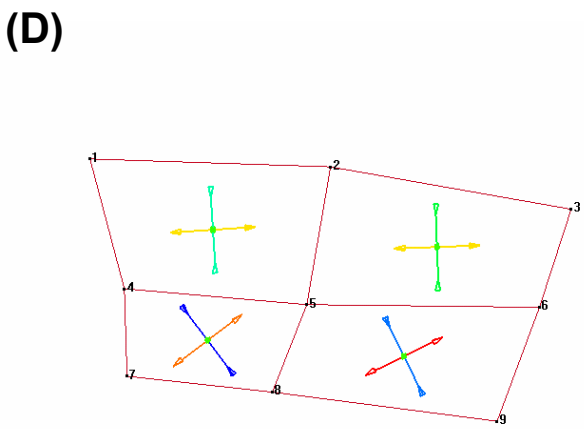
(D)